Sampling Density-Adaption for Directly Filtered Projection Reconstruction

A. M. Nagel[1], F. B. Laun[1], C. Matthies[1], A. Biller[2,3], and M. Bock[1]
[1]Medical Physics in Radiology, German Cancer Research Center, Heidelberg, Germany, [2]Radiology, German Cancer Research Center, Germany, [3]Department of Diagnostic and Interventional Radiology, University Hospital Heidelberg, Germany

Introduction

For ^{23}Na-MRI large voxel sizes (2 - 5 mm)^3 are required, which can lead to Gibbs' ringing artifacts that markedly degrade image quality. One approach to minimize ringing artifacts is the use of an appropriate apodization function (e.g., a Hamming-window). Due to the fast transversal relaxation time T_2^* of ^{23}Na, pulse sequences with short echo times like 3D projection reconstruction (3DPR) and twisted projection imaging (3D-TPI) (1) are favorable. It was already shown for 3D-TPI, that a sampling density that matches the desired filter function (sampling density weighted apodization [SW]) provides higher SNR compared to uniform k-space sampling with post-acquisition filtering apodization [UPF] (2). Although 3D-TPI acquires a given FOV within a shorter time compared to 3D projection reconstruction (3DPR) (3,4), the latter is often preferred due to smaller gradient slew rate requirements and a less complicated implementation of the k-space trajectories. Therefore, in this work a sampling density weighted apodization was implemented for conventional 3DPR trajectories (3DPR-SW).

Methods

3DPR-SW ^{23}Na-images were acquired on a 3 T and a 7 T whole body scanner (Magnetom TIM Trio, Magnetom 7 T, Siemens Medical Solutions, Erlangen, Germany) using double-resonant (^{23}Na/^{1}H) quadrature birdcage coils (Rapid Biomed GmbH, Rimpar, Germany). To use the sampling density of a Hamming-window (Fig. 1a; (5)) the gradient amplitude of the 3DPR-SW sequence was varied after a time t_0, and a fraction p of the k-space radius (Fig. 1b).

The 3DPR-SW sequence was compared with two post-acquisition filtered 3DPR-sequences, a conventional 3DPR-sequence (3DPR-PF) and a sampling density adapted sequence with uniform sampling density (3DPR-UPF) (4). Depending on the sampling scheme k-space positions are reached at different times (Fig. 1c), and T_2^* relaxation thus affects the point-spread functions (PSF). To quantify the T_2^*-related blurring, the PSFs FWHM were calculated with different ratios of T_{RO}/T_2* for all three sequences.

To evaluate the performance of the sequences, brain images were acquired with the following parameters: 3T-images (Fig. 2a): TE = 0.2 ms; TR = 21 ms; T_{RO} = 16.7 ms; α = 55°; 32000 projections; resolution: (2.7 mm)^3. 7T-images (Fig. 2b,c): TE = 0.5 ms; TR = 25 ms; T_{RO} = 20 ms; α = 55°, 32000 projections; resolution: (2.5 mm)^3. 7T-images (Fig. 2d): TE = 0.55 ms; TR = 9 ms; T_{RO} = 5 ms; α = 36°, 32000 projections; 2 averages; resolution: (2.5 mm)^3. The readout gradient parameters and the corresponding radial fractions p are shown in table 1.

Results and Discussion

The FWHM of the PSF are shown in Fig. 1d) for all three sequences. The 3DPR-UPF-sequence shows the smallest FWHM, and thus only minor blurring artifacts are expected, which is in good agreement with the in-vivo brain images (Fig. 2). SNR values for brain tissue are shown in table 1. The 3DPR-PF sequence shows the lowest SNR-values and is most prone to artifacts from B_0-inhomogeneities. The 3DPR-SW sequence has the highest SNR-values and shows a smaller "noise speckle size" compared to the 3DPR-UPF sequence (Fig. 2a).

In regions with B_0-inhomogenieties such as the eyes (red arrow) and the paranasal sinuses (blue arrow) (Fig. 2c), blurring and distortions degrade image quality in particular for the 3DPR-PF-sequence. Here, the 3DPR-UPF-sequence shows the best results, since k-space is traversed more rapidly (Fig. 1c) than with 3DPR and 3DPR-SW so that less phase is accumulated for a given k-space position. At shorter readout length (T_{RO} = 5 ms) these artifacts are negligible for all three sequences (Fig. 2d) and slightly higher SNR-values for the 3DPR-SW-sequence were measured (Tab. 1).

Both 3DPR-UPF and 3DPR-SW show a much better performance than the conventional 3DPR-PF. Comparing the 3DPR-SW- and the 3DPR-UPF-sequence, the SNR-benefits of the 3DPR-SW approach must be weighed against the better artifact-behavior of the post-filtered technique. For a short readout time of T_{RO} = 5 ms, B_0-inhomogeneity artifacts and blurring are negligible and the use of the 3DPR-SW-sequence is beneficial.

References

1. Boada et al. Magn Reson Med 1997; 37(5):706-715
2. Stobbe et al. Magn Reson Med 2008; 60(4):981-986
3. Boada et al. Magn Reson Med 1997; 37(3):470-477
4. Nagel et al. Magn Reson Med; doi:10.1002/mrm.22157 (2009)
5. Harris F. Proc. IEEE 1978: 66: 51-181

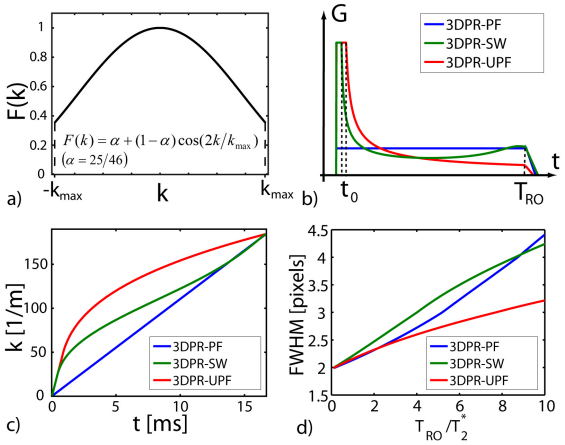

Fig. 1: a) Hamming-window. b) Readout gradients and c) radial k-space positions versus time of the different sequences. b) FWHM of the PSFs. b-d) Parameters used as in Fig. 2a (s. Tab. 1).

Table 1: Parameters of the readout gradients for the images in Fig. 2 and measured SNR-values for brain tissue.

	3DPR-PF			3DPR-SW			3DPR-UPF		
figure	*2a*	*2b,c*	*2d*	*2a*	*2b,c*	*2d*	*2a*	*2b,c*	*2d*
G [mT/m]	0.98	0.89	3.57	5	4.81	14.0	5	4.81	16.9
t_0 [µs]	-	-	-	462	500	240	867	946	340
p	1	1	1	0.14	0.13	0.16	0.26	0.25	0.28
SNR	7	14	9	10	20	10	7	16	9

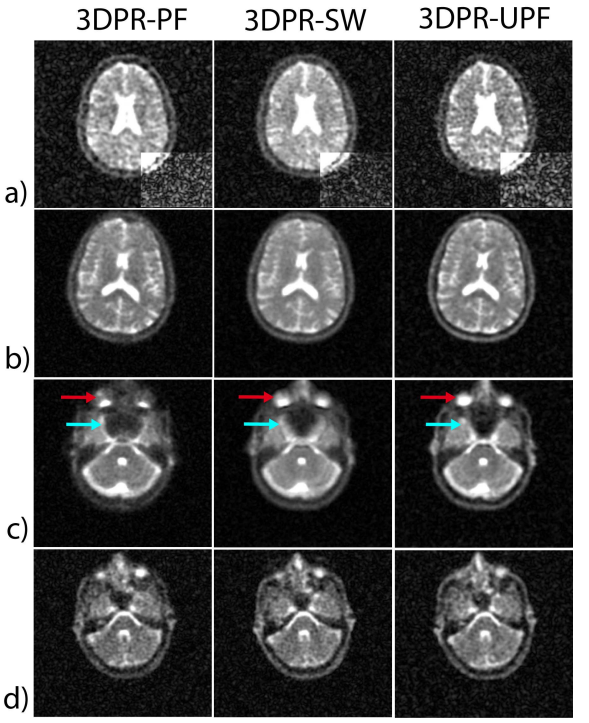

Fig. 2: Brain ^{23}Na-images acquired with the three different sequences. a) 3T images. The right lower part of the image was scaled to highlight to noise. The 3DPR-PF and the 3DPR-SW images show a reduced speckle size when compared the DA-3DPR-PF image. b) c) 7T images, exemplary slices of 3D data set. d) 7T images with short readout length (T_{RO} = 5 ms).